Food Hydrocolloids 152 (2024) 109842

Contents lists available at ScienceDirect

Food Hydrocolloids

journal homepage: www.elsevier.com/locate/foodhyd

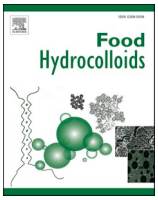

Foaming and structural properties of egg yolk components microgel particles and their adsorption characteristics at the air-water interface

Jiahan Liu [a], Yuemeng Wang [b], Yuxin Zou [a], Yue Wu [a], Wenle Guan [a], Jianrong Yang [a,**], Xin Li [a,*]

[a] School of Life Sciences, Yantai University, Yantai, Shandong, 264005, PR China
[b] School of Food and Biological Engineering, Yantai Institute of Technology, Yantai, Shandong, 264003, PR China

ARTICLE INFO

Keywords:
Microgel particles from egg yolk components
Adsorption capacity
Foam properties
Interfacial properties
Microstructure

ABSTRACT

In this study, microgel particles of egg yolk and its components were constructed by inducing and modifying their structure via the high-pressure homogenization (HPH). In order to compare their structural characterization and reveal their adsorption mechanism at the air-water interface, yolk components were also combined with egg white protein (EWP) to achieve their microgels for investigation. Results suggested that after HPH, foam stabilities of egg yolk protein microgel (EYM) and egg yolk plasma microgel (EPM) were significantly improved, whereas no significance occurred on egg yolk granules microgel (EGM). Interestingly, after HPH, the adsorption capacity of the microgels from combination of yolk components and EWP exhibited a significant increasing trend. However, their interfacial adsorption stability was poor. Fluorescence spectrum and surface tension revealed that more hydrophilic groups and lower surface tension would occur on EY and EP after HPH, whilst no significant effects would happen on EG, which was consistent with the results of foaming characteristics. SDS-PAGE exhibited that there was no obvious change in the protein bands of egg yolk and its components, indicating that egg yolk and component proteins did not undergo covalent crosslinking or degradation with HPH treatment. In summary, our study prepares for the first time of the microgel particles from egg yolk components for stabilizing the air-water interface. In addition, we have revealed the relationship between the physicochemical properties, microstructures and interfacial adsorption properties of the microgel particles from egg yolk components, and have explored their mechanisms in depth.

1. Introduction

Foam is a two-phase colloidal structure in which gases are dispersed in a liquid, semi-liquid or solid continuous phase (Dabestani & Yeganehzad, 2019a). Foam is widely used in various aerated systems in daily life, such as beer, milk, cream, cakes and bread, which are popular with consumers (Kruk, Ptaszek, & Kaczmarczyk, 2021; Murray, 2020). However, from a thermodynamic perspective, foam constitutes an unstable system characterized by a significant surface free energy present at the air-water interface (Wouters, et al., 2018). In order to reduce the interfacial area, foams are prone to coarsening, coalescence and disproportionation during processing and storage, resulting in unstable product properties mainly in foam systems (Horozov, 2008). Due to the demand for large-scale use of foams in various commercial sectors, stabilizers such as silicone polyether emulsions and non-ionic surfactants are commonly used at this stage to improve foam stability by reducing interfacial tension and preventing bubble coalescence (X. Zhang, Zhao, & He, 2020). However, most of these stabilizers are non-edible, and their long-term use may pose health risks such as allergic reactions, toxicity, *etc*. In addition, they cannot be directly applied in the food field. Therefore, developing methods to improve foam stability and constructing safe and edible foam stabilizers is crucial for the current food field to ensure product quality, shelf life, and consumer safety.

As one of the most effective and natural protein sources, the edible part of eggs could be divided into egg white and egg yolk. Egg white protein is an important animal protein with exceptional foaming properties and is extensively used in bakery products (Sheng, et al., 2018). Egg yolk, which is nutritionally dense and structurally intricate, is rich in proteins, essential fatty acids, phospholipids, and vitamins *etc*. (Liu,

* Corresponding author. School of Food Sciences, Yantai University, Shandong, PR China.
** Corresponding author.
E-mail addresses: edelweissyjr@163.com (J. Yang), nallyxin@163.com (X. Li).

https://doi.org/10.1016/j.foodhyd.2024.109842
Received 1 December 2023; Received in revised form 28 January 2024; Accepted 30 January 2024
Available online 13 February 2024

et al., 2023). After centrifugation, egg yolk can be easily split into two main components: the supernatant, known as egg yolk plasma (EP), and the sedimentary layer, referred to as egg yolk granules (EG) (Marcet, Álvarez, Paredes, & Díaz, 2014). The primary proteins in egg yolk and its components (EP and EG) are lipoproteins, which have a challenging time being separated from both the protein and lipid fractions. Thus, in turn, significantly impacts their foaming properties, rendering their ability to adsorb stably at the air-water interface highly compromised (J. Li, Li, et al., 2018). In the actual processing and production situations, it's inevitable for egg white to get contaminated by egg yolk due to various reasons such as the poor quality of eggs and manual operation errors. The resulting lipoprotein residues can significantly undermine the foamability and foam stability of egg white protein, thus limiting its application in food systems (Li, Wang, Sun, Lv, & Yang, 2021; G. WANG & WANG, 2010).

To establish a lipoprotein interfacial stabilization system and to investigate the stabilization mechanism, a special structure is required to enhance the foam stability. In fact, it has been suggested that the functional properties of proteins may be linked to the formation of condensed proteins networks and surface-active stabilizing particles (Gtari, Aschi, Nicolai, & Freitas, 2016). Therefore, we may speculate that a similar relationship could exist for active particles adsorbed at the air-water interfacial layer, indicating that protein particles may play a greater role in improving foam ability and foam stability. In recent years, there has been a growing interest in the development of foam stabilizers for food-grade solid particles, such as microgel particles derived from egg white protein (Chang, et al., 2016), sea bass protein (L. Zhang et al., 2022), peanut protein (Jiao, Shi, Wang, & Binks, 2018), soy protein (Matsumiya & Murray, 2016), and zein protein (Dai, et al., 2018), which have demonstrated Pickering-type stability of foams and emulsions. While scholars seem to be more inclined to focus on the oil-water interface, there have been limited investigation on the air-water interface. It has been demonstrated that microgel particles can stabilize emulsions,but there have been few studies on their application for foam stabilization using egg white protein microgel particles (Li, Yang, Murray, & Sarkar, 2020). This is insufficient for foams, and lipoprotein microgel particles are even rarer. Therefore, the interfacial adsorption mechanism remains unclear, necessitating in-depth investigations.

To expand the application range of lipoproteins as a foam stabilizer, this study aims to develop microgel particles from egg yolk and its components. The objective is to characterize the physicochemical, foaming, interfacial and structural properties of these microgel particles compared to untreated EY/EP/EG. The ultimate goal is to reveal the adsorption mechanism of lipoproteins at the air-water interface, and constructing an edible foam stabilizer.

2. Materials and methods

2.1. Materials

Fresh chicken eggs were purchased from New World Department Store (Yantai, China). Bovine Serum Albumin V (BSA-V) was obtained from Solarbio Science & Technology Co., Ltd. (Beijing, China). Sodium dodecyl sulfate (SDS) was purchased from Beyotime Biotechnology Co., Ltd. (Shanghai, China). Other reagents used in this study were supplied by McLean reagent company and analytical grade.

2.2. Sample preparation

2.2.1. Preparation of egg white protein solution

Egg white was extracted from egg yolk with a separator, and then homogenized under a magnetic stirrer (500 r/min speed) for 1 h to get the egg white protein (EW) without further processing.

2.2.2. Preparation of egg yolk and its components

According to previous method with minor modifications (X. Li, Li, et al., 2018), yolk membrane was pricked with a tweezer and the egg yolk liquid was diluted with deionized water at a ratio of 1:1.5 (w/w) and adjusted to pH 7.0 with 1 N NaOH. Afterwards, the diluted yolk liquid was homogenized at a lower speed (200 r/min) for 2 h. After equilibrating overnight at 4 °C, egg yolk liquid was centrifuged for 45 min at 4 °C (10,000×*g*) to obtain two kinds of components, including the supernatant, *i.e.*, egg yolk plasma (EP) and the precipitate, *i.e.*, egg yolk granules (EG).

2.2.3. Preparation of microgel particles from egg yolk components

Microgel particles from egg yolk (EY) and its components were prepared via a top-down approach of preparing of a heat-set protein hydrogel by high-pressure homogenization, followed by Li, Murray, Yang, and Sarkar (2020a) with some modifications. Briefly, EY and EG were diluted 1:1 (w/w) with deionized water and heated at 90 °C for 30 min in a water bath, while EP was adopted at the same condition without dilution. The gels were diluted to 3 wt% and broken up into pieces, then passed (three times) through the high-pressure homogenizer at 400 MPa. The sample solutions were labeled as egg yolk microgel particles (EYM), egg yolk plasma microgel particles (EPM) and egg yolk granules microgel particles (EGM), respectively. The preparation steps are shown in Fig. 1.

2.3. Measurement of particle size and zeta potential

The particle size and zeta potential of sample solutions were measured by a Nano Brook 90 plus instrument (Brookhaven, USA). The sample solutions were diluted to 0.01% with deionized water and their particle size were measured at a 90° scattering angle. Then, the sample solutions were diluted to 0.001% to determine their zeta potential. All the measurements were performed in triplicate at 25 °C.

2.4. Measurement of soluble protein content

2.4.1. Production of standard curve

The soluble protein contents of sample solutions were determined by the Biuret method (Chen & Kuo, 2016). The standard curve was made by BSA-V. Blank control was prepared without BSA-V solution and the absorbance values of solutions in each tube were measured using a UV-spectrophotometer (UV-5100, Shanghai METASH Instruments Co., Ltd., China) at 540 nm. The addition amount of BSA-V solution, deionized water and Biuret reagent is shown in the Supplementary Material.

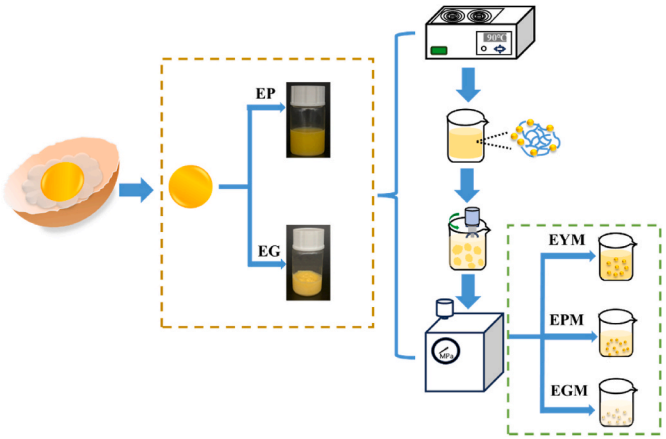

Fig. 1. Schematic illustration of preparation of egg yolk and its component microgel particles.

2.4.2. Measurement of sample solutions

The sample solutions were centrifuged at 5000 r/min at 25 °C for 20 min with a centrifuge, then 1 mL supernatant was mixed with 4 mL Biuret reagent and stood for 30 min. The A_{540} of the sample solutions were measured, and their corresponding protein milligrams were checked on the standard curve, which was the content of the measured protein solution (mg/mL).

2.5. Measurement of fluorescence spectrum

The fluorescence spectrum of sample solutions was analyzed by a RF-6000 fluorescence spectrophotometer (Shimadzu Co., Japan). All the samples were diluted to 0.1%. The excitation light wavelength was 280 nm, the scanning wavelength was 290–500 nm, and the slit width was 5 nm.

2.6. Measurement of foam properties

2.6.1. Foam capacity

Foam capacity of sample solutions was indicated by overrun in this experiment. Foams were produced by stirring sample solutions (total amount was 30 g) with an eggbeater for 2 min. After that, a spatula was used to level the top of foams and recorded the foam volume (Li, Wang, Lv, & Yang, 2022). The overrun was calculated by Eq. (1):

$$\text{Overrun}\ (\%) = \frac{100 \times (m_i - m_f)}{m_f} \quad (1)$$

where: m_i is the mass of unwhipped sample solution; m_f is the mass after whipping of the same volume of the unwhipped sample solution.

2.6.2. Foam stability

Foam stability of samples was indicated by drainage in this experiment. The above whipped foams were placed for 30 min at 25 °C. The drainage fluid was gently decanted and weighted (Kuropatwa, Tolkach, & Kulozik, 2009), which was calculated by Eq (2):

$$\text{Drainage}\ (\%) = \frac{100 \times m_d}{m_f} \quad (2)$$

where: m_d is the mass of drainage; m_f is the mass of foams.

2.6.3. Microstructure of foams

The fresh generated foams and the coarsened foams after 30 min were separately spread on a glass slide to observe their microstructure via a Reb-BL forward-inverted integrated fluorescence microscope (ECHO, USA) (The microscope magnification was 4×).

2.7. Viscosity of sample solutions

Viscosity of sample solutions was detected using a MARS 40 rotational rheometer (Thermo Fisher Scientific Co., Germany) according to the previous method (Chang, et al., 2017). A plate with a diameter of 35 mm was selected for the measurement. Sample solutions were appended to the stage and the gap between two plates was set to 1 mm, and the shear rate was increasing from 0.1 to 100 s^{-1}.

2.8. Surface tension of sample solutions

The surface tension of sample solutions was determined via a DCAT-25 surface tensiometer (Data Physics Co., Germany). Dip the plate into the sample solutions and click the start button to measure the surface tension of the samples. (Zhao, et al., 2021a). The measuring range of the instrument was 1–2000 mN/m. The plate width was 19.9 mm, the plate thickness was 0.2 mm, and the plate retraction speed was set to be 1.00 mm/s. The standard deviation was within ±0.03 mN/m.

2.9. Sodium dodecyl sulfate–polyacrylamide gel electrophoresis

Sodium dodecyl sulfate–polyacrylamide gel electrophoresis (SDS-PAGE) was analyzed according to the previous method (Q. Li, Wang, et al., 2022). The acrylamide stacking and separating gels were 5% and 12%, respectively. The samples were mixed with buffer (samples: buffer = 4:1, v/v) and heated at 100 °C for 5 min. Protein markers were used as control. After the electrophoretic gel was stained with Coomassie brilliant blue solution, decolorization was performed in a solution containing acetic acid, methanol and water (10:40:50, v/v/v) until the strips were clear.

2.10. Scanning electron microscopy (SEM)

The microstructure of samples was observed via a SEM (JSM-7610F, JEOL Ltd., Tokyo, Japan), where the samples were freeze-dried via a vacuum freeze-dryer and their powders were imaged at an acceleration voltage of 2 kV (Fuertes, et al., 2017). Before that, powders were fixed on the metal sample platforms through the conductive double-sided tape and gold-plated with the ion sputtering coater.

2.11. Fourier transform infrared spectroscopy (FTIR)

FTIR spectroscopy was employed to analyze the secondary structures of proteins in the samples (Yu, et al., 2022). Freeze-dried sample powders were mixed with KBr evenly, then they were pressed into thin slices. The spectra were scanned with a IRAffinity-1 FTIR spectrometer (Shimadzu Co., Japan) in the wavelength region of 4000–400 cm^{-1} at a resolution of 1 cm^{-1}. The infrared spectral data and the secondary structures were analyzed using the OMNIC software version 9.7 and PeakFit software version 4.12.

2.12. Statistical analyses

All experiments were performed in triplicate and SPSS software version 26.0 was used to analyze the obtained data. The results were statistically reported by drawing with software Origin 2021.

3. Results and discussion

3.1. Physicochemical properties of microgel particles from egg yolk components

3.1.1. Particle size and zeta potential

Table 1 presents the outcomes of particle size, polydispersity index (PDI) and zeta potential of diverse sample solutions. As can be seen in Table 1, natural egg yolk and its components exhibit greater particle size due to their significant lipid content. Notably, the application of HPH treatment resulted in a significant reduction in particle size for the sample solutions (EYM/EPM/EGM). This finding suggests that HPH treatment facilitates the intermolecular fracture and dispersion of lipids and proteins in EY/EP/EG through the consistent application of high-

Table 1
Particle size, PDI and zeta potential of sample solutions under high-pressure homogenization (HPH) treatment, including EY (egg yolk), EP (egg yolk plasma), EG (egg yolk granules) and EYM (egg yolk protein microgel particles), EPM (egg yolk plasma microgel particles) and EGM (egg yolk granules microgel particles).

sample solutions	particle size (nm)	PDI	zeta potential (mV)
EY	1725.79 ± 37.87^{a}	0.39 ± 0.01^{a}	-14.76 ± 0.19^{ab}
EP	1643.75 ± 55.30^{b}	0.13 ± 0.10^{c}	-14.31 ± 0.89^{a}
EG	605.23 ± 10.73^{c}	0.29 ± 0.01^{b}	-16.23 ± 0.39^{b}
EYM	459.69 ± 56.28^{d}	0.28 ± 0.07^{b}	-22.03 ± 0.74^{c}
EPM	422.77 ± 2.70^{d}	0.30 ± 0.01^{ab}	-22.46 ± 0.62^{c}
EGM	424.50 ± 5.59^{d}	0.34 ± 0.00^{ab}	-26.28 ± 1.26^{d}

speed shear and pressure (SIRVENTE, et al., 2007). This process subjects the samples to high pressure, leading to deformation and movement that generates a turbulence effect during the homogenization process, ultimately forming a stable and homogeneous dispersed system. The average size distribution of these samples falls within the range of 300 nm–500 nm, which is considered an appropriate particle size range for microgel (Gaillard, et al., 2023).

The width of the particle size distribution for the samples was captured by PDI, which ranges from 0 to 1 (Boonlao, Shrestha, Sadiq, & Anal, 2020). The lower PDI value (0.1–0.25) indicates a comparatively narrow size distribution, while values exceeding 0.5 denote a significantly broader distribution (Tamjidi, Shahedi, Varshosaz, & Nasirpour, 2014). Table 1 reveals that the PDI values of EYM/EPM/EGM exceeded 0.25, suggesting that the HPH treatment resulted in a broader range of particle size distributions within the samples.

Surface charge is a crucial indicator of electrostatic interactions between reactive protein molecules (Junhua Li et al., 2019). As illustrated in Table 1, the zeta potential values of EYM/EPM/EGM increased significantly compared to untreated egg yolk and its components. This finding suggests that HPH treatment modifies intermolecular electrostatic interactions and triggers structural alterations in the proteins, leading to the gradual exposure of negatively charged amino acid groups. This exposure subsequently causes an elevation in the zeta potential values of EYM, EPM and EGM.

3.1.2. Soluble protein content

Fig. 2A displays the standard curve for the determination of soluble protein content in samples. According to the standard curve, the linear regression equation was derived as $y = 0.4657–0.0002$, with an R^2 value of the standard curve = 0.9999. The high R^2 value indicates a strong linear correlation, validating the use of this standard curve for subsequent experiments.

The soluble protein content of samples is presented in Fig. 2B, including the natural egg yolk components (EY/EP/EG) and yolk components treated with HPH (EYM/EPM/EGM). As shown in Fig. 2B, the soluble protein content of EP and EG were significantly decreased compared to EY, which may have been due to increased electrostatic interactions between the components after centrifugation of the egg yolk. Interestingly, when EY and EG were subjected to HPH treatment, the soluble protein content of EYM and EGM decreased. This may be attributed to the complex structure of EY and EG, and the HPH treatment led to a decrease in the solubility of EY and EG, increasing the content of insoluble proteins in them. However, the soluble protein content in EPM was clearly increased. This can be attributed to the large amount of low-density lipoprotein (LDL) in EP, which had high solubility properties, and HPH treatment may have enhanced the contact of LDL with water molecules, leading to an increase in the soluble protein content of EPM (He, et al., 2023). In summary, proteins in egg yolk and its components are denatured by HPH treatment, but the effect of the treatment was still dependent on the type of protein, such as LDL with high solubility leads to an increase of soluble proteins in EP after HPH treatment, whereas insoluble HDL leads to decrease of soluble proteins in EG after HPH treatment.

3.1.3. Fluorescence spectrum

Fluorescence spectra is an effective method to detect changes in protein tertiary structure (Y. Q. Wang, Zhang, Zhang, Tao, & Tang, 2007). Fig. 3 shows the fluorescence intensity of egg yolk and its components after HPH treatment, as the wavelength (λ) changes. It is evident that the fluorescence intensities of EYM and EPM were significantly enhanced and redshifted after HPH treatment, indicating that the proteins in EY and EP were denatured after HPH treatment. The aromatic amino acid groups were gradually exposed to the aqueous solution, leading to an increase in the polarity of the environment in which they were located, and the fluorescence emission peaks of the proteins (λ_{max}) were also elevated. However, the fluorescence intensity of EGM was

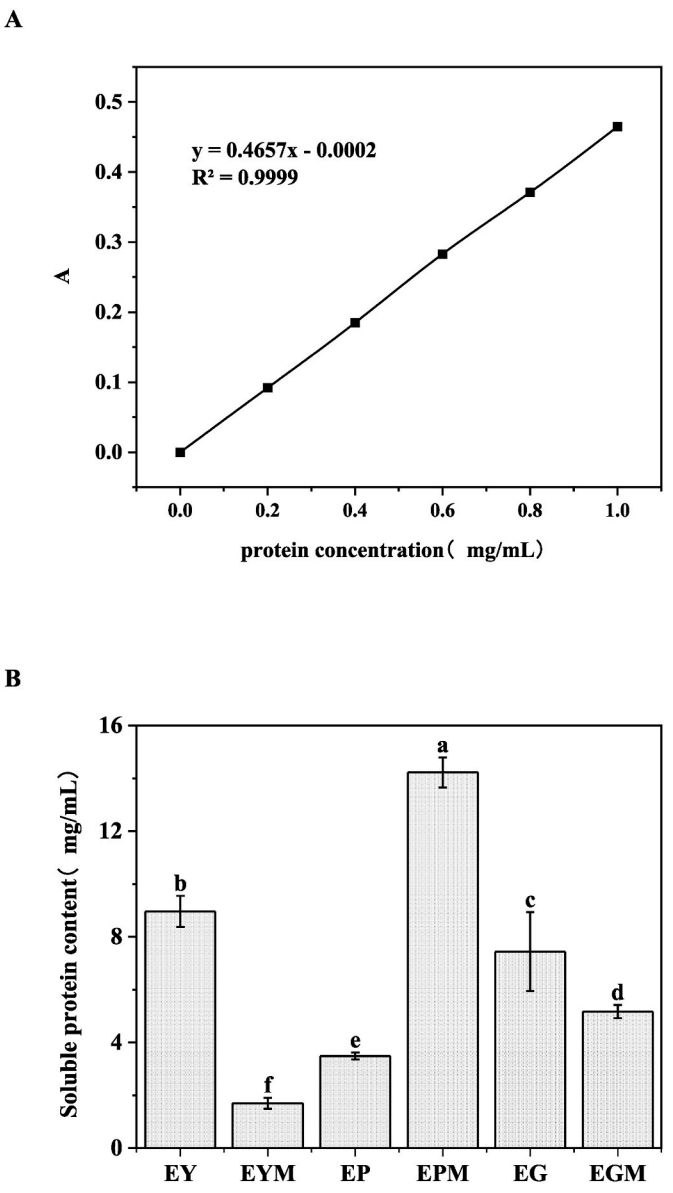

Fig. 2. The standard curve for the determination of soluble protein content (A) and soluble protein content of egg yolk components and their microgel particles, including EY (egg yolk), EP (egg yolk plasma), EG (egg yolk granules) and EYM (egg yolk protein microgel particles), EPM (egg yolk plasma microgel particles) and EGM (egg yolk granules microgel particles) (B).

reduced after HPH treatment, with no significant change in the peak protein fluorescence emission. This might be attributed to the more complex structure of EG, which exists mainly in the form of insoluble high-density lipoproteins and phosvitin (HDL - PV) complexes connected by calcium phosphate bridges to form a dense network structure (T. StrixnerJ, & KulozikGebhardt, 2014). Therefore, HPH treatment may not result in a change in the protein tertiary structure of EG, and its fluorescence spectrum was not redshifted or blueshifted.

3.2. Foaming properties of microgel particles from egg yolk components

3.2.1. Adsorption capacity of egg yolk and its component microgel particles at the air-water interface

To clarify the impact of HPH treatment on the adsorption capacity of egg yolk and its components at the air-water interface, we individually whipped all samples (EY/EP/EG/EYM/EPM/EGM), as shown in Fig. 4A. Neither EG nor EGM exhibited foamability when stirred separately.

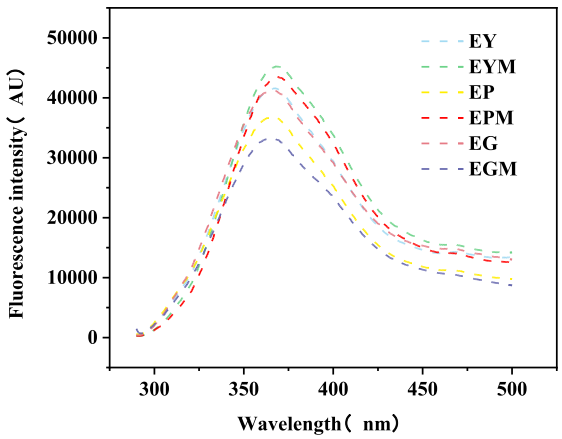

Fig. 3. Fluorescence spectrum of egg yolk components and their microgel particles, including EY (egg yolk), EP (egg yolk plasma), EG (egg yolk granules) and EYM (egg yolk protein microgel particles), EPM (egg yolk plasma microgel particles) and EGM (egg yolk granules microgel particles).

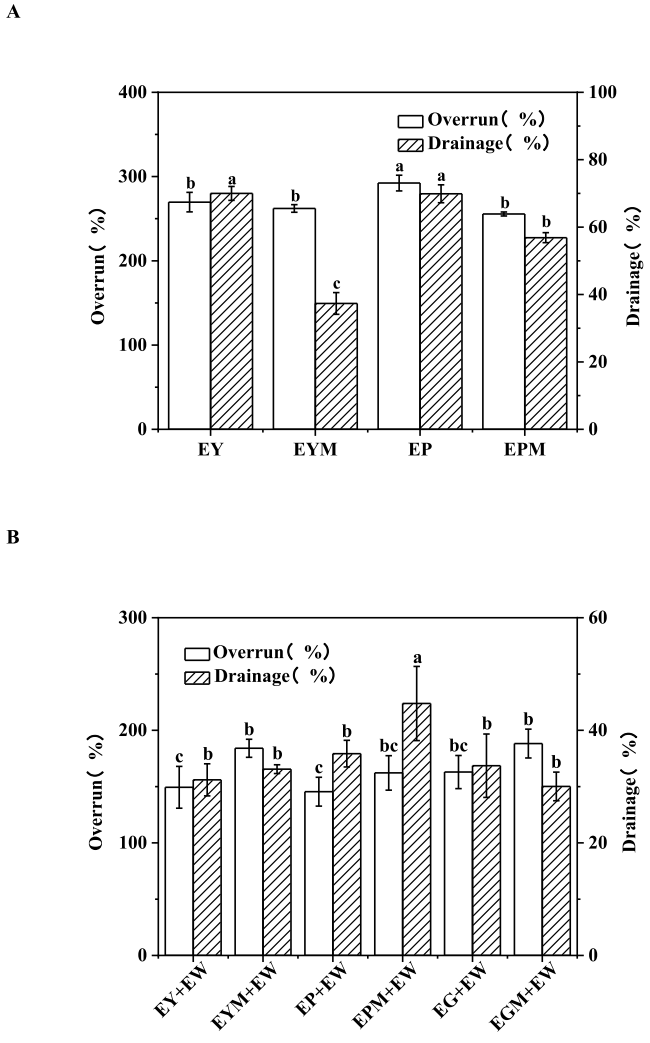

Fig. 4. Foam properties of microgel particles from egg yolk components. (A) Foam capability (overrun) and foam stability (drainage) of EY, EP and EYM, EPM; (B) Foam capability (overrun) and foam stability (drainage) of egg white (EW) with egg yolk components and with their microgel particles.

Therefore, they were not shown in Fig. 4A. At a protein concentration of 3 wt%, natural EY and EP were observed to possess superior foam ability but inferior foam stability. This was attributed to the substantial amount of free fat in EY and EP, which could rapidly adsorb at the air-water interface and form a protein-oil film, resulting in a superior foamability. However, this structure was found to be highly unstable, and the ability to stabilize the foam was slightly lacking. Therefore, the foam stability of natural EY and EP decreased when left for 30 min (X. Li, Li, et al., 2018).

HPH treatment not only denatured the proteins in the samples but also induced fatty acid aggregation in the samples, which reduced the free fatty acid content. This resulted in a decrease in adsorption capacity and a slower rate of adsorption, but an increase in stabilization capacity at the air-water interface. As a result, the foam stability of EYM and EPM was improved to a certain extent, although their foam abilities were decreased. EGs are natural micro- and nano-aggregates assembled from proteins and lipids, containing a large amount of HDL and a high solid content (Yang, et al., 2020). The dense structure of lipoproteins resulted in issues such as slow interfacial adsorption and insufficient interfacial adsorption capacity. A combination of fluorescence spectroscopy (Fig. 3) and surface tension (Fig. 7) revealed that HPH treatment did not significantly modify EG lipoproteins, leading to neither EG nor EGM exhibiting foamability when stirred separately. Furthermore, the whipping method was a crucial determinant of the samples' foaming ability. Currently, common whipping methods included hand-shaking and mechanical stirring, *etc.*, each technique leading to distinct foam abilities (Dabestani & Yeganehzad, 2019b; Li, Murray, Yang, & Sarkar, 2020b). In this study, mechanical stirring was used, which may not be suitable for whipping EG. Therefore, future exploration is required to improve EG's adsorption capacity at the air-water interface.

In order to reveal the interfacial adsorption properties of microgel particles from egg yolk and its components after interaction with EW, we added all the samples (EY/EP/EG/EYM/EPM/EGM) to EW at a ratio of 1% (Fig. 4B). Intriguingly, after mixing with EW, the foam ability and foam stability of EYM and EPM exhibited an opposite trend to that of Fig. 4A. These results might be ascribed to the fact that when EYM/EPM were compounded with EW, the lipoproteins in EYM/EPM showed a competitive relationship with EW, enhancing the adsorption capacity of lipoprotein-EW at the air-water interface, thereby improving the foam ability of the samples. However, the interfacial stability was reduced, leading to lower foam stability. Notably, both EG and EGM exhibited high whipping properties when combined with EW, particularly after the interactions between EGM and EW. The foam ability and foam stability were improved compared to the other samples (EYM/EPM with EW). Gaillard et al. (2023) suggested that ultra-high-pressure homogenization would have a significant impact on the disruption of the large and dense aggregates present in EG into smaller particles, which could result in the formation of a more homogeneous network structure. This may have been the main reason for the enhanced foam ability and foam stability of the complex system of EGM and EW.

3.2.2. *Microstructure of foams*

The foam structure and bubble distribution of four sample solutions (EY/EP/EYM/EPM) are presented in Fig. 5A. As can be observed in this figure, the bubble sizes of EYM and EPM were smaller and the bubble distribution was more uniform compared to EY and EP. This phenomenon corresponds to the results of particle size analysis.

Gas diffusion is the process of smaller bubbles transforming into larger bubbles, which reduces the number of smaller bubbles while increasing the size and collapse of larger bubbles (Huang, et al., 2017; X. Li, Li, et al., 2018). Fig. 5B shows the foam structure and bubble distribution of four sample solutions (EY/EP/EYM/EPM) after being placed for 30 min. As can be seen, the bubble sizes of all sample solutions exhibited an enlarging trend, especially for EY and EP. Additionally, the bubble shapes of EY and EP were more irregular and polyhedral, while the bubble shapes of EYM and EPM were more rounded. This result was

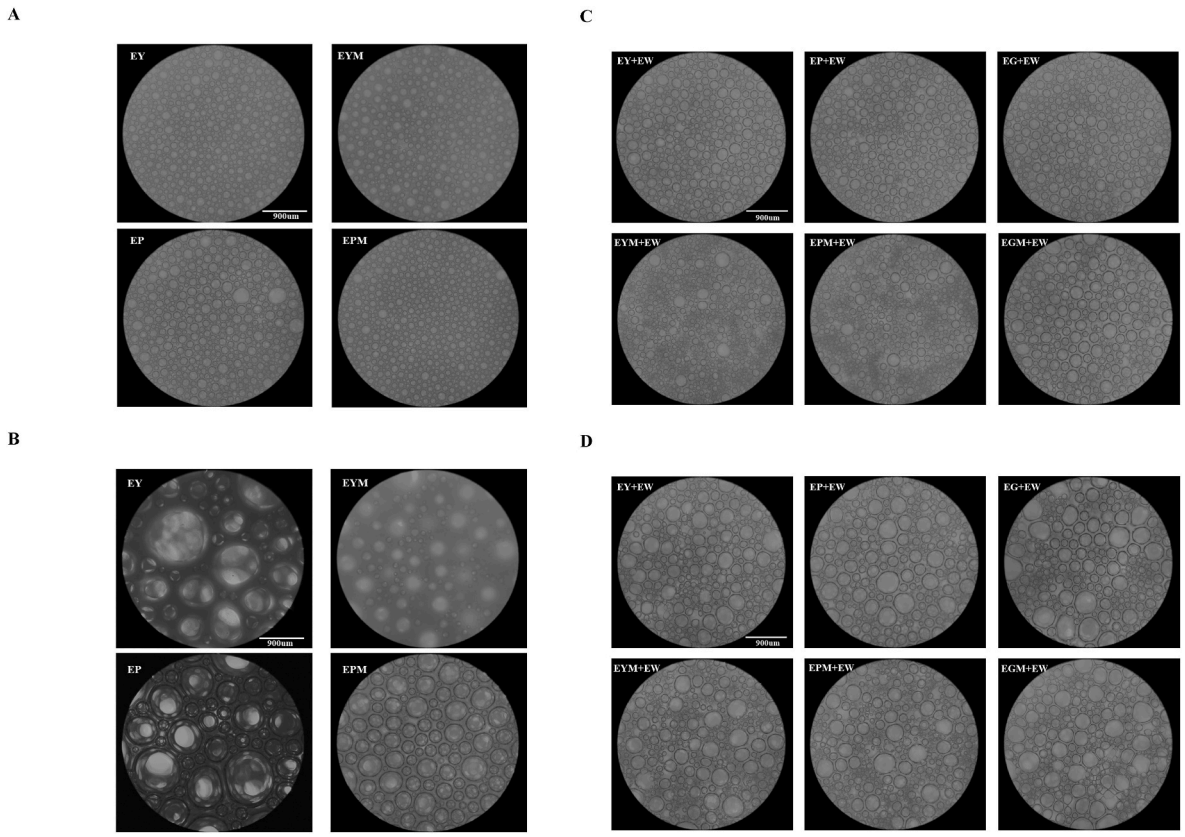

Fig. 5. Optical micrographs of foams stabilized by egg yolk components and their microgel particles as a function of time (A: unwhipped foams of EY, EYM, EP and EPM; B: foams of EY, EYM, EP and EPM after left for 30 min), as well as those stabilized by yolk components/microgel particles and EW (C: unwhipped foams of EW with EY, EW with EP, EW with EG, EW with EYM, EW with EPM and EW with EGM; D: foams of EW with EY, EW with EP, EW with EG, EW with EYM, EW with EPM and EW with EGM after left for 30 min) (4 ×).

consistent with the foam stability (drainage) results presented in Fig. 4A, which further confirms that the HPH treatment improved the foam stability of the samples.

Structure of foams and bubble distribution for EW with different egg yolk components (EY/EYM/EP/EPM/EG/EGM) are shown in Fig. 5C and D. As can be seen in Fig. 5C, the foam distribution of systems of EYM/EPM/EGM with EW after whipping was less uniform and the foam size was slightly different. When the samples were placed for 30 min, the bubble size of the EYM with EW composite system was larger than that of the EY with EW composite system, and the bubble distribution of the EPM with EW composite system was more uneven than that of the EP with EW composite system. In contrast, the foam of the composite system of EGM with EW had a more rounded shape and a more uniform distribution than the foam of the composite system of EG with EW. These observations are consistent with the results presented in Fig. 4B. The above phenomena suggest that the size, morphology and distribution of bubbles can serve as indicators of the foam stability of samples (Dimitrova, Petkov, Kralchevsky, Stoyanov, & 2017). The larger the bubble size, irregular morphology and uneven distribution, the poorer the foam stability of the sample.

3.3. *Interfacial properties of microgel particles from egg yolk components*

3.3.1. *Viscosity properties*

The apparent viscosity is generally considered to be a crucial factor for foaming stability (Akhtar, Ahmed, Elgaddafi, Shah, & Amani, 2018). Fig. 6 shows the apparent viscosity results for the different samples. As shown in Fig. 6, all sample solutions exhibited pseudoplastic fluid behavior, with a decrease in viscosity with increasing shear rate (Veronica Giacintucci, Mattia, Sacchetti, Neri, & Pittia, 2016).Another

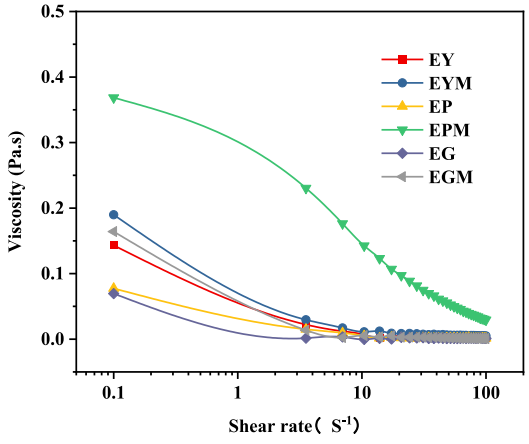

Fig. 6. Viscosity of egg yolk components and their microgel particles, including EY (egg yolk), EP (egg yolk plasma), EG (egg yolk granules) and EYM (egg yolk protein microgel particles), EPM (egg yolk plasma microgel particles) and EGM (egg yolk granules microgel particles).

aspect, the apparent viscosities of EYM/EPM/EGM were increased after HPH treatment. This result indicated that HPH treatment leads to emulsification of fat globules and denaturation of proteins with the formation of a large number of lipid-protein complexes, which is an important reason for the increase in apparent viscosity. In addition, in combination with Fig. 4A, although the foam stability of the samples can

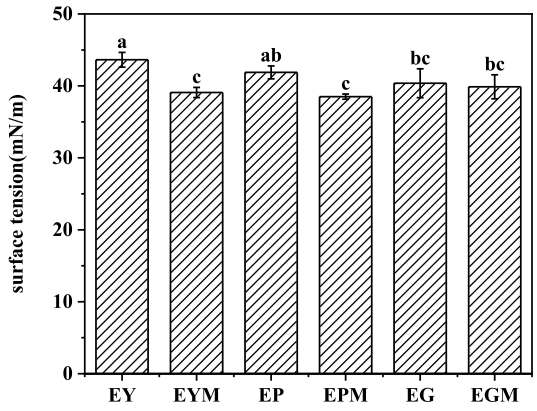

Fig. 7. Surface tension of egg yolk components and their microgel particles, including EY (egg yolk), EP (egg yolk plasma), EG (egg yolk granules) and EYM (egg yolk protein microgel particles), EPM (egg yolk plasma microgel particles) and EGM (egg yolk granules microgel particles).

be indicated by the increase in apparent viscosity, it seems that for EG, the apparent viscosity does not directly reflect its foaming ability. Therefore, the adsorption of EG at the air-water interface still needs to be explored in the future.

3.3.2. Surface tension

Surface tension is an important indicator for assessing the rate of protein adsorption and unfolding at the air-water interface, which further determines the foaming ability of proteins (Zhao, et al., 2021b). Fig. 7 illustrates the surface tension changes in the control and HPH-treated samples. As seen in Fig. 7, compared to the untreated egg yolk and its components, the surface tension values of EYM and EPM decreased, while there was no significant difference observed for EGM. Theoretically, a decrease in protein surface tension enhances the foaming ability of proteins. However, when whipping EYM and EPM, a slightly reduced foaming ability was observed (Fig. 4A). It was speculated that HPH treatment caused the protein molecules in EY and EP to combine with water to form a more stable emulsion system for better emulsification. However, the stabilization of air bubbles was not sufficient, resulting in no significant increase in foamability for EYM and EPM. On the other hand, the surface tension of EG remained unchanged due to its intricate network structure, indicating that HPH treatment might not significantly affect it. This result aligns with the fluorescence spectroscopy results (Fig. 3) and foam ability (overrun) results (Fig. 4A). In summary, it is evident that while surface tension can offer insights into protein adsorption at the air-water interface, it cannot solely determine protein foaming ability, which is instead influenced by a range of factors.

3.4. Structural properties of microgel particles from egg yolk components

3.4.1. SDS-PAGE

The effect of HPH treatment on the SDS-PAGE pattern of egg yolk and its components is shown in Fig. 8. The SDS-PAGE pattern was used to compare in detail the protein bands of different samples, including EY/EYM/EP/EPM/EG/EGM. Based on the results shown in the SDS-PAGE patterns, eight clear protein bands with molecular weights ranging from 14.3 to 200.0 kDa could be observed in each of the sample systems. The bands in each lane were well explained by the protein subunits contained in each sample system. According to previous research (Naderi, House, & Pouliot, 2014), the electrophoretic bands of egg yolk protein had a wide range of molecular weight distribution and

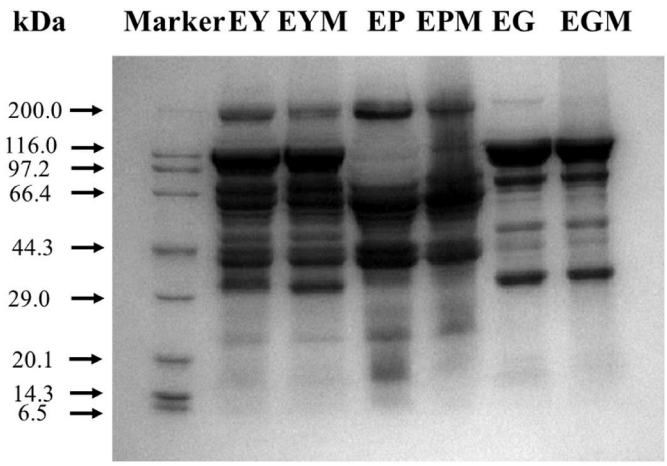

Fig. 8. SDS-PAGE of egg yolk components and their microgel particles, including EY (egg yolk), EP (egg yolk plasma), EG (egg yolk granules) and EYM (egg yolk protein microgel particles), EPM (egg yolk plasma microgel particles) and EGM (egg yolk granules microgel particles).

consisted of 16 bands with molecular weights between 14.4 and 200 kDa. EP was rich in LDL and bands at 175, 130, 105, 85, 70, 65, 50 and 15 kDa had been reported to indicate LDL (Xu, et al., 2019). The large amounts of HDL and phosvitin were present in EG, and the apo molecular weights of HDL were predominantly distributed at 110, 80, 47, and 32 kDa. The phosvitin had two protein bands, α-phosvitin and β-phosvitin, with molecular weights corresponding to 40 kDa and 45 kDa, respectively (Naderi, et al., 2014). As can be seen in Fig. 8, there was no obvious change in the protein bands of samples, which indicates that the HPH treatment did not cause covalent crosslinking of proteins in the samples. Moreover, the study reported by Xie et al. (2020) showed that the bands of egg yolk proteins were not significantly changed by high-intensity ultrasonic treatment. It can be seen that the molecular weight of the proteins in the egg yolk and fractions might not be changed by a single physical modification, which could be explained by the cross-linking or degradation/fracture of the proteins have not been compromised. In the future, we can try to combine physical modification techniques with other techniques to explore the structure and properties of lipoproteins more deeply, so as to further elucidate the adsorption of lipoproteins at the air-water interface.

3.4.2. SEM analysis

To further elucidate the effect of the HPH treatment on the microstructure of egg yolk and its components, we investigated the surface morphology of all samples (EY/EYM/EP/EPM/EG/EGM) using scanning electron microscopy (SEM), which is shown in Fig. 9. For natural egg yolk component samples (EY/EP/EG), a dense structure with a large average particle size was observed. When the samples were subjected to HPH, it could be observed that the aggregation state of the samples were changed, with large aggregates being dispersed into small particles and the particle size of the samples (EYM/EPM/EGM) being significantly reduced. Meanwhile, the results of SEM images also reconfirmed that the HPH treatment can effectively act on the complex structure of egg yolk and its components, resulting in the depolymerization and dispersion of the proteins in egg yolk and components (EY/EP/EG). This result corresponds to the particle size results in Table 1.

3.4.3. Changes in the secondary structure of sample systems

FTIR analysis was conducted to investigate the effect of HPH treatment on the secondary structure of egg yolk and components proteins. Fig. 10 shows the spectra of all sample systems in the entire region of 4000–500 cm^{-1} (Fig. 10A) and in the region of the amide I band (1600 -1700 cm^{-1}) (Fig. 10B). As can be seen in Fig. 10A, the characteristic

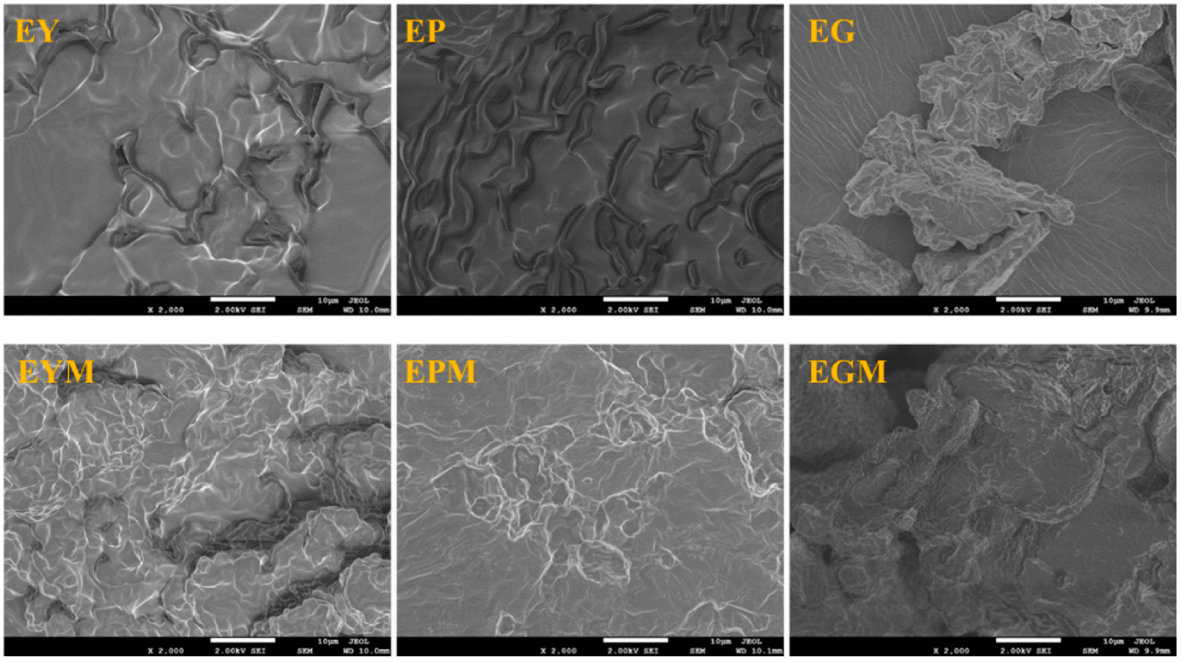

Fig. 9. SEM images of egg yolk components and their microgel particles. (A) EY (egg yolk) and EYM (egg yolk protein microgel particles); (B) EP (egg yolk plasma) and EPM (egg yolk plasma microgel particles); (C) EG (egg yolk granules) and EGM (egg yolk granules microgel particles).

peaks of each sample were slightly shifted between 2800 and 3000 cm^{-1} and 1600 -1800 cm^{-1}. The peak at 2926 cm^{-1} corresponds to the anti-symmetric stretching vibration of -CH2, the peak at 2855 cm^{-1} to the symmetric stretching vibration of -CH2, and the peak at 1745 cm^{-1} to the stretching vibration of –C═O ester bond (Krilov, Balarin, Kosovic, Gamulin, & Brnjas-Kraljevi, 2009). All three absorption peaks indicated that lipids were the most abundant component of egg yolk, which was in agreement with previous studies (Xie, et al., 2020). The main component of the amide I region (1600-1700 cm^{-1}) is generated by C = O stretching vibrations, and this region is affected by hydrogen bonding and thus contains rich secondary structure information of proteins (Matheus, Friess, & Mahler, 2006). We performed detailed calculations on this region and the results are shown in Fig. 10B.

To further understand the changes of protein structures in different sample systems, the percentage of protein secondary structures were calculated and presented in Fig. 10B. The amide I region (1600-1700 cm^{-1}) is the most informative part of the FTIR spectrum regarding the secondary structure of proteins, which mainly consists of α-helix (1660-1651 cm^{-1}), random-coil (1650-1641 cm^{-1}), β-sheet (1640-1610 cm^{-1}), and β-turn (1700-1661 cm^{-1}) (Long, et al., 2015). As shown in Fig. 10B, the percentages of β-sheet in EYM decreased while the percentages of β-sheet in EPM and EGM increased slightly upon HPH treatment. Previous studies have shown that increased β-sheet leads to aggregation of protein (Guerrero, Kerry, & Caba, 2014). Therefore, it can be concluded in this study that proteins aggregation in EP and EG was increased by HPH treatment. Additionally, the increase in α-helix and the decrease in random-coil were strongly associated with the charge carried by the protein (X. Li, Wang, et al., 2022). The α-helix contains more hydrogen bonds, and an increase in the homo-charge carried by the protein will break the hydrogen bonds, resulting in a decrease in the α-helix structure. Based on the trend in Fig. 10B, we can infer that EP might contain a large number of homogeneous charges, explaining why the α-helix structure of EPM was significantly reduced after HPH treatment. It can be seen that HPH treatment could be change the secondary structure and functional groups in the molecules of egg yolk proteins. However, further studies are needed to clarify the underlying mechanisms.

4. Conclusion

The impact of HPH treatment on the physicochemical, foaming, interfacial and structural properties of egg yolk and its components were explored in this study. The findings showed that HPH treatment led to a significant increase in the soluble protein content of EPM. When it came to the foam properties, EYM and EPM lipoproteins could be stably adsorbed at the gas-water interface after HPH treatment. When the samples (EYM/EPM/EGM) were intercalated with EW, the foam ability of lipoprotein-EW was significantly improved, but the stability of EYM-EW and EPM-EW at the air-water interface decreased. Based on these results, we can preliminarily conclude that the egg yolk fraction that is closest to EY in nature may be EP. The SEM results showed that after treated with HPH, the morphologies of the samples (EYM/EPM/EGM) were uniformly distributed in the form of small particles. Furthermore, the secondary structure of the proteins was also altered with HPH treatment. However, further studies are still needed.

In summary, this study demonstrated that a kind of green and healthy food-grade foam stabilizer could be successfully prepared by using HPH technology. The findings also reveal the competitive adsorption mechanisms of these stabilizers at the air-water interface, which holds significant importance in the development of food-grade interfacial stabilized protein systems. This discovery paves the way of further exploration of HPH technology's potential in food science and provides a foundation for future research in this area.

CRediT authorship contribution statement

Jiahan Liu: Writing – original draft, Methodology, Investigation, Formal analysis, Data curation, Conceptualization. **Yuemeng Wang:** Writing – review & editing, Software, Methodology. **Yuxin Zou:** Writing – review & editing, Formal analysis. **Yue Wu:** Writing – review & editing, Methodology. **Wenle Guan:** Methodology, Formal analysis. **Jianrong Yang:** Writing – review & editing, Supervision, Resources, Methodology. **Xin Li:** Writing – review & editing, Supervision, Project administration, Funding acquisition, Data curation, Conceptualization.

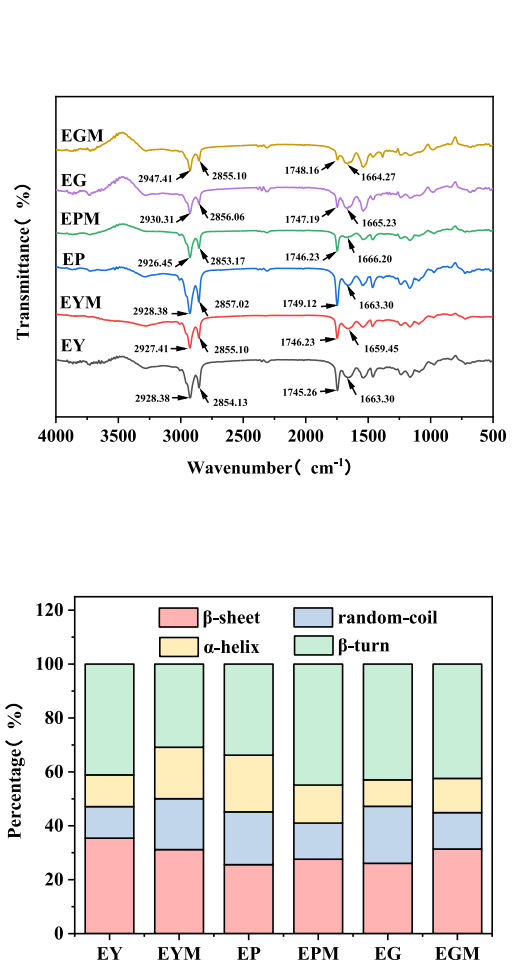

Fig. 10. FTIR spectra of microgel particles from egg yolk components; (A) Spectra of egg yolk and its component microgel particles in the region of 4000–500 cm^{-1}; (B) Secondary structure of egg yolk components and their microgel particles.

Declaration of competing interest

We confirm that the work is original and has not been published elsewhere, nor is currently under consideration for publication elsewhere. We have no conflicts of interest to disclose the content of this paper. No conflict with the funding source or financial contributions supported this work.

Data availability

Data will be made available on request.

Acknowledgement

The authors would like to thank for the financial support from the Natural Science Foundation of Shandong Province (ZR2021QC065) and the Postgraduate Research and Innovation Fund Program of Yantai University (GGIFYTU2356).

Appendix A. Supplementary data

Supplementary data to this article can be found online at https://doi.org/10.1016/j.foodhyd.2024.109842.

References

Akhtar, T. F., Ahmed, R., Elgaddafi, R., Shah, S., & Amani, M. (2018). Rheological behavior of aqueous foams at high pressure. *Journal of Petroleum Science and Engineering, 162*, 214–224.
Boonlao, N., Shrestha, S., Sadiq, M. B., & Anal, A. K. (2020). Influence of whey protein-xanthan gum stabilized emulsion on stability and in vitro digestibility of encapsulated astaxanthin. *Journal of Food Engineering, 272*, Article 109859.
Chang, C., Li, J., Li, X., Wang, C., Zhou, B., Su, Y., et al. (2017). Effect of protein microparticle and pectin on properties of light mayonnaise. *LWT - Food Science and Technology, 82*, 8–14.
Chang, C., Niu, F., Gu, L., Li, X., Yang, H., Zhou, B., et al. (2016). Formation of fibrous or granular egg white protein microparticles and properties of the integrated emulsions. *Food Hydrocolloids, 61*, 447–486.
Chen, S.-Y., & Kuo, M.-I. (2016). Physicochemical and functional properties of Chinese soft-shell turtle (Pelodiscus sinensis) egg. *Food Research International, 85*, 36–43.
Dabestani, M., & Yeganehzad, S. (2019a). Effect of Persian gum and Xanthan gum on foaming properties and stability of pasteurized fresh egg white foam. *Food Hydrocolloids, 87*, 550–560.
Dabestani, M., & Yeganehzad, S. (2019b). Effect of Persian gum and Xanthan gum on foaming properties and stability of pasteurized fresh egg white foam. *Food Hydrocolloids, 87*, 550–560.
Dai, L., Zhan, X., Wei, Y., Sun, C., Mao, L., McClements, D. J., et al. (2018). Composite zein - propylene glycol alginate particles prepared using solvent evaporation: Characterization and application as Pickering emulsion stabilizers. *Food Hydrocolloids, 85*, 281–290.
Dimitrova, L. M., Petkov, P. V., Kralchevsky, P. A., Stoyanov, S. D., & E, G. P. (2017). Production and characterization of stable foams with fine bubbles from solutions of hydrophobin HFBII and its mixtures with other proteins. *Colloids and Surfaces A: Physicochemical and Engineering Aspects, 521*, 92–104.
Fuertes, S., Laca, A., Oulego, P., Paredes, B., Rendueles, M., & Díaz, M. (2017). Development and characterization of egg yolk and egg yolk fractions edible films. *Food Hydrocolloids, 70*, 229–239.
Gaillard, R., Gagnon, D., Perreault, V.e., Marciniak, A., Pouliot, Y., Brisson, G., et al. (2023). Effect of ultra-high pressure homogenization on structural and techno-functional properties of egg yolk granule proteins. *LWT-food Science & Technology, 178*, Article 114624.
Giacintucci, V., Mattia, C. D., Sacchetti, G., Neri, L., & Pittia, P. (2016). Role of olive oil phenolics in physical properties and stability of mayonnaise-like emulsions. *Food Chemistry, 213*(15), 369–377.
Gtari, W., Aschi, A., Nicolai, T., & Freitas, R. A.d. (2016). Core-shell particles formed by ?-lactoglobulin microgel coated with xyloglucan. *International Journal of Biological Macromolecules, 92*, 357–361.
Guerrero, P., Kerry, J. P., & Caba, K.d. l. (2014). FTIR characterization of protein–polysaccharide interactions in extruded blends. *Carbohydrate Polymers, 111*, 598–605.
He, X., Wang, J., Wang, Y., Wang, B., Zhang, J., & Geng, F. (2023). Quantitative lipidomic analysis of egg yolk, yolk granule, and yolk plasma. *Journal of Food Composition and Analysis, 115*, Article 104880.
Horozov, T. S. (2008). Foams and foam films stabilised by solid particles. *Current Opinion in Colloid & Interface Science, 13*(3), 134–140.
Huang, T., Z-c, T., Wang, H., X, S., Zhang, L., Niu, P., et al. (2017). Promotion of foam properties of egg white protein by subcritical water pre-treatment and fish scales gelatin. *Colloids and Surfaces A: Physicochemical and Engineering Aspects, 512*, 171–177.
Jiao, B., Shi, A., Wang, Q., & Binks, B. P. (2018). High internal phase pickering emulsions stabilized solely by peanut protein microgel particles with multiple potential applications. *Angewandte Chemie, 57*(30), 9274–9278.
Krilov, D., Balarin, M., Kosovic, M., Gamulin, O., & Brnjas-Kraljevi, J. (2009). FT-IR spectroscopy of lipoproteins—a comparative study. *Spectrochimica Acta Part A: Molecular and Biomolecular Spectroscopy, 73*(4), 701–706.
Kruk, J., Ptaszek, P., & Kaczmarczyk, K. (2021). Technological aspects of xanthan gum and gum Arabic presence in chicken egg albumin wet foams: Application of nonlinear rheology and nonparametric statistics. *Food Hydrocolloids, 117*, Article 106683.
Kuropatwa, M., Tolkach, A., & Kulozik, U. (2009). Impact of pH on the interactions between whey and egg white proteins as assessed by the foamability of their mixtures. *Food Hydrocolloids, 23*(8), 2174–2181.
Li, X., Li, J., Chang, C., Wang, C., Zhang, M., Su, Y., et al. (2018a). Foaming characterization of fresh egg white proteins as a function of different proportions of egg yolk fractions. *Food Hydrocolloids, 90*, 118–125.
Li, X., Murray, B. S., Yang, Y., & Sarkar, A. (2020a). Egg white protein microgels as aqueous Pickering foam stabilizers: Bubble stability and interfacial properties. *Food Hydrocolloids, 98*, Article 105292.
Li, X., Murray, B. S., Yang, Y., & Sarkar, A. (2020b). Egg white protein microgels as aqueous Pickering foam stabilizers: Bubble stability and interfacial properties. *Food Hydrocolloids, 98*, 105292.105291-105292.105210.
Li, J., Wang, C., Li, X., Su, Y., Yang, Y., & Yu, X. (2018b). Effects of pH and NaCl on the physicochemical and interfacial properties of egg white/yolk. *Food Bioscience, 23*, 115–120.
Li, X., Wang, Y., Lv, J., & Yang, Y. (2022). Investigations of foaming, interfacial and structural properties of dispersions, batters and cakes formed by industrial yolk-contaminated egg white protein. *LWT-Food Science & Technology*, (154), Article 112776.

Li, X., Wang, Y. M., Sun, C. F., Lv, J. H., & Yang, Y. J. (2021). Comparative study on foaming properties of egg white with yolk fractions and their hydrolysates. *Foods, 10*(9), 2238.
Li, X., Yang, Y., Murray, B. S., & Sarkar, A. (2020). Combination of egg white protein and microgels to stabilize foams: Impact of processing treatments. *Journal of Food Engineering, 275*, Article 109860.
Li, J., Yang, Y., Su, Y., Gu, L., Chang, C., & Yang, Y. (2019). Phase separation in ternary composite cold-set gel of egg yolk/κ-carrageenan/xanthan: Study on rheological and proton mobility properties. *LWT - Food Science and Technology, 116*, Article 108497.
Li, Q., Zhang, X., Tang, S., Mi, S., Lu, L., Zeng, Q., et al. (2022). Improved effect of ultrasound-assisted enzymolysis on egg yolk powder: Structural properties, hydration properties and stability characteristics. *Food Chemistry, 15*, 382.
Liu, Y., Wang, K., Ma, J., Wang, Z., Zhu, Q., & Jin, Y. (2023). Effect of yolk spheres as a key histological structure on the morphology, character, and oral sensation of boiled egg yolk gel. *Food Chemistry, 424*, Article 136380.
Long, G., Ji, Y., Pan, H., Sun, Z., Li, Y., & Qin, G. (2015). Characterization of thermal denaturation structure and morphology of soy glycinin by FTIR and SEM. *International Journal of Food Properties, 18*(4), 763–774.
Marcet, I., Álvarez, C., Paredes, B., & Díaz, M. (2014). Inert and oxidative subcritical water hydrolysis of insoluble egg yolk granular protein, functional properties, and comparison to enzymatic hydrolysis. *Journal of Agricultural and Food Chemistry, 62*(32), 8179–8186.
Matheus, S., Friess, W., & Mahler, H.-C. (2006). FTIR and nDSC as analytical tools for high-concentration protein formulations. *Pharmaceutical Research, 23*(6), 1350–1363.
Matsumiya, K., & Murray, B. S. (2016). Soybean protein isolate gel particles as foaming and emulsifying agents. *Food Hydrocolloids, 60*, 206–215.
Murray, B. S. (2020). Recent developments in food foams. *Current Opinion in Colloid & Interface Science, 50*, Article 101394.
Naderi, N., House, J. D., & Pouliot, Y. (2014). Scaling-up a process for the preparation of folate-enriched protein extracts from hen egg yolks. *Journal of Food Engineering, 141*(85–92).
Sheng, L., Wang, Y., Chen, J., Zou, J., Wang, Q., & Ma, M. (2018). Influence of high-intensity ultrasound on foaming and structural properties of egg white. *Food Research International, 108*, 604–610.
Sirvente, H., Beaumal, V., Gaillard, C., Bialek, L., Hamm, D., & Anton, M. (2007). Structuring and functionalization of dispersions containing egg yolk, plasma and granules induced by mechanical treatments. *Food Chemistry, 55*(23), 9537–9544.
Strixner, T., J, S., Kulozik, U., & Gebhardt, R. (2014). Structural study on hen-egg yolk high density lipoprotein (HDL) granules. *Food Biophysics, 9*(4), 314–321.
Tamjidi, F., Shahedi, M., Varshosaz, J., & Nasirpour, A. (2014). EDTA and a-tocopherol improve the chemical stability of astaxanthin loaded into nanostructured lipid carriers. *European Journal of Lipid ence and Technology, 116*(8), 968–977.
Wang, G., & Wang, T. (2010). Effects of yolk contamination, shearing, and heating on foaming properties of fresh egg white. *Journal of Food Science, 74*(2), C147–C156.
Wang, Y. Q., Zhang, H. M., Zhang, G. C., Tao, W.-H., & Tang, S.-H. (2007). Interaction of the flavonoid hesperidin with bovine serum albumin: A fluorescence quenching study. *Journal of Luminescence, 126*(1), 211–218.
Wouters, A. G. B., Rombouts, I., Fierens, E., Brijs, K., Blecker, C., Delcour, J. A., et al. (2018). Foaming and air-water interfacial characteristics of solutions containing both gluten hydrolysate and egg white protein. *Food Hydrocolloids, 77*, 176–186.
Xie, Y., Wang, J., Wang, Y., u, D.i. W., Liang, D., Ye, H., et al. (2020). Effects of high-intensity ultrasonic (HIU) treatment on the functional properties and assemblage structure of egg yolk. *Ultrasonics Sonochemistry, 60*, Article 104767.
Xu, L., Zhao, Y., Xu, M., Yao, Y., Wu, N., Du, H., et al. (2019). Changes in physico-chemical properties, microstructure, protein structures and intermolecular force of egg yolk, plasma and granule gels during salting. *Food Chemistry, 275*, 600–609.
Yang, Y., Zhao, Y., Xu, M., Yao, Y., Wu, N., Du, H., et al. (2020). Effects of strong alkali treatment on the physicochemical properties, microstructure, protein structures, and intermolecular forces in egg yolks, plasma, and granules. *Food Chemistry, 311*(1), 1–10.
Yu, Z., Hu, J., Gao, S., Han, R., Ma, L., & Chen, Y. (2022). Joint effects of enzymatic and high-intensity ultrasonic on the emulsifying propertiesof egg yolk. *Food Research International, 156*, Article 11146.
Zhang, L., Zaky, A. A., Zhou, C., Chen, Y., Su, W., Wang, H., et al. (2022). High internal phase Pickering emulsion stabilized by sea bass protein microgel particles: Food 3D printing application. *Food Hydrocolloids, 131*, Article 107744.
Zhang, X., Zhao, N., & He, C. (2020). The superior mechanical and physical properties of nanocarbon reinforced bulk composites achieved by architecture design–a review. *Process in Materials Science, 113*, Article 100672.
Zhao, Q., Ding, L., Xia, M., Huang, X., Isobe, K., Handa, A., et al. (2021a). Role of lysozyme on liquid egg white foaming properties: Interface behavior, physicochemical characteristics and protein structure. *Food Hydrocolloids, 120*(4), Article 106876.
Zhao, Q., Ding, L., Xia, M., Huang, X., Isobe, K., Handa, A., et al. (2021b). Role of lysozyme on liquid egg white foaming properties: Interface behavior, physicochemical characteristics and protein structure. *Food Hydrocolloids, 120*(4), Article 106876.